BBA - Molecular Basis of Disease 1863 (2017) 3117–3127

Contents lists available at ScienceDirect

BBA - Molecular Basis of Disease

journal homepage: www.elsevier.com/locate/bbadis

Inhibition of Drp1-mediated mitochondrial fission improves mitochondrial dynamics and bioenergetics stimulating neurogenesis in hippocampal progenitor cells from a Down syndrome mouse model

Daniela Valenti[a,*], Leonardo Rossi[b], Domenico Marzulli[a], Francesco Bellomo[c], Domenico De Rasmo[a], Anna Signorile[d], Rosa Anna Vacca[a,*]

[a] Institute of Biomembranes, Bioenergetics and Molecular Biotechnologies, National Council of Research, Bari, Italy
[b] Department of Clinical and Experimental Medicine, University of Pisa, Italy
[c] Division of Nephrology and Dialysis, Bambino Gesù Children's Hospital - IRCCS, Rome, Italy
[d] Department of Basic Medical Sciences, Neuroscience and Sense Organs, University of Bari, Italy

ARTICLE INFO

Keywords:
Down syndrome
Mitochondrial dysfunction
Hippocampal neurogenesis
Mitochondrial network
Drp1
Mdivi-1

ABSTRACT

Functional and structural damages to mitochondria have been critically associated with the pathogenesis of Down syndrome (DS), a human multifactorial disease caused by trisomy of chromosome 21 and associated with neurodevelopmental delay, intellectual disability and early neurodegeneration. Recently, we demonstrated in neural progenitor cells (NPCs) isolated from the hippocampus of Ts65Dn mice -a widely used model of DS - a severe impairment of mitochondrial bioenergetics and biogenesis and reduced NPC proliferation. Here we further investigated the origin of mitochondrial dysfunction in DS and explored a possible mechanistic link among alteration of mitochondrial dynamics, mitochondrial dysfunctions and defective neurogenesis in DS. We first analyzed mitochondrial network and structure by both confocal and transmission electron microscopy as well as by evaluating the levels of key proteins involved in the fission and fusion machinery. We found a fragmentation of mitochondria due to an increase in mitochondrial fission associated with an up-regulation of dynamin-related protein 1 (Drp1), and a decrease in mitochondrial fusion associated with a down-regulation of mitofusin 2 (Mnf2) and increased proteolysis of optic atrophy 1 (Opa1). Next, using the well-known neuroprotective agent mitochondrial division inhibitor 1 (Mdivi-1), we assessed whether the inhibition of mitochondrial fission might reverse alteration of mitochondrial dynamics and mitochondrial dysfunctions in DS neural progenitors cells. We demonstrate here for the first time, that Mdivi-1 restores mitochondrial network organization, mitochondrial energy production and ultimately improves proliferation and neuronal differentiation of NPCs. This research paves the way for the discovery of new therapeutic tools in managing some DS-associated clinical manifestations.

1. Introduction

Down syndrome (DS), the most frequent genetic cause of intellectual disability, is due to either full or partial trisomy of chromosome 21. Clinically, DS is a neurodevelopmental disease characterized by neural developmental delay with impairment in language, learning and memory associated with an atypical craniofacial profile and increased susceptibility to congenital heart defects, immune and metabolic disorders [1,2]. The majority of patients reaching middle age, develop symptoms of premature aging and neurochemical features of the Alzheimer's disease and related dementia associating DS as a neurodegenerative disease [3]. On this basis, the pathogenesis of DS has been deeply investigated in the hope of increasing our understanding of the DS neurobiology and identifying efficacious drug targets to improve the clinical phenotype.

A growing body of literature has shown that structural and functional damages to mitochondria are critically associated with DS pathogenesis and are inherent features of DS (for refs see [4,5]). Of note, mitochondrial dysfunctions are also involved in the pathogenesis of others intellectual disability-related diseases, such as Rett syndrome

Abbreviations: AR, aspect ratio; BrdU, bromodeoxyuridine; CaN, calcineurin; DAPI, 4',6-diamidino-2-phenylindole; DCX, doublecortin; Drp1, dynamin-related protein 1; DS, Down syndrome; L-Opa, long Opa1; Mdivi-1, mitochondrial division inhibitor 1; Mnf2, mitofusin 2; NPCs, neural progenitor cells; OLIGO, oligomycin; Opa1, optic atrophy 1; OXPHOS, oxidative phosphorylation; P-Drp1, S637-phosphorylated Drp1; RCAN1, regulator of calcineurin 1; S-Opa, short Opa1; wt, wild-type

* Corresponding authors at: Institute of Biomembranes, Bioenergetics and Molecular Biotechnologies, National Council of Research, Via Amendola 165/A, 70126 Bari, Italy.
E-mail addresses: d.valenti@ibiom.cnr.it (D. Valenti), r.vacca@ibiom.cnr.it (R.A. Vacca).

http://dx.doi.org/10.1016/j.bbadis.2017.09.014
Received 13 July 2017; Received in revised form 11 September 2017; Accepted 18 September 2017
Available online 20 September 2017
0925-4439/

and autism (for refs see [4,6]), and neurodegenerative conditions, including Alzheimer's and Parkinson's diseases (for refs see [7]).

In DS, impairment in respiratory capacity, mitochondrial membrane potential and ATP production have been demonstrated in mitochondria of peripheral cells, obtained from DS subjects [8–12], and of central nervous system cells from mouse models of DS [13,14]. Alterations of mitochondrial morphology and dynamics have also been recently reported in human fetal fibroblasts with chromosome 21trisomy [15].

We recently analyzed mitochondrial functions in neural progenitor cells (NPCs) isolated from the hippocampus of Ts65Dn mice, a widely used model of DS, which recapitulates many major brain structural and functional phenotypes of the syndrome, including impaired hippocampal neurogenesis [16,17]. We found that, in Ts65Dn NPCs, mitochondrial bioenergetics and mitochondrial biogenic program were strongly compromised and that molecules able to restore oxidative phosphorylation (OXPHOS) efficiency and mitochondrial biogenesis can also improve NPC proliferation [18,19].

There is growing evidence of a close relationship between functional mitochondrial bioenergetics and mitochondrial network integrity [20,21], especially in the cells of the central nervous system in which mitochondria are synthesized in the soma and must travel along axons and dendrites [22]. Mitochondria continuously and reversibly rearrange their structure assuming elongated or punctiform distribution in the processes of fusion and fission, respectively [23]. These processes are regulated by highly conserved GTPase-dependent proteins, such as dynamin-related protein 1 (Drp1) and fission 1 (Fis1) for fission and mitofusin 1 (Mfn1), mitofusin 2 (Mfn2), and optic atrophy 1 (Opa1) for fusion [23,24]. An altered balance between fission and fusion leads to structural and functional abnormalities in the mitochondria network and, ultimately, to an impairment in neuronal function. Indeed, in several neurodegenerative diseases the maintenance of mitochondrial dynamics is required for neural development processes and synaptic formation and reorganization (for refs see [25]).

Very relevant is that overexpression of the human regulator of calcineurin 1 (RCAN1) promotes deregulation of Drp1 activity associated with an increase of mitochondrial fission, mitochondrial dysfunction, oxidative stress and early age-dependent memory and synaptic plasticity deficits in mice [26]. Based on these evidences and since RCAN1 protein, encoded by the 21q22.1-q22.2 region of human chromosome 21, is overexpressed in Down syndrome [27,28], we argued that Drp1 could be deregulated in DS and Drp1-mediated mitochondrial fission could promote mitochondrial damage and alter hippocampal neurogenesis.

In the present study, we explored whether Drp1-dependent mitochondrial fragmentation occurred in hippocampal NPCs. We tested the effects of the mitochondrial division inhibitor 1 (Mdivi-1), a selective inhibitor of Drp1 [29], on mitochondrial network, mitochondrial functions and NPC proliferation and differentiation. Mdivi-1 has been shown to exert neuroprotective effects in several cell and animal model systems [30–32] and recently proposed as drug against neurodegeneration and brain injury [33,34]. The current work aims to determine a possible mechanistic link among alteration of mitochondrial dynamics, mitochondrial dysfunctions and defective neurogenesis in DS.

2. Materials and methods

2.1. Adult hippocampal NPCs cultures

NPC lines isolated from the dentate gyrus of adult (6–8 weeks) Ts65Dn mice (male and female carrying a partial trisomy of chromosome 16) or wild-type (wt) littermates, were a gift of Dr. Andrea Contestabile of the “Istituto Italiano di Tecnologia”, Genoa, Italy [17].

Cells were cultured as a monolayer on poly-D-lysine (PDL; Sigma-Aldrich) and laminin-coated (Roche) flasks in Neurobasal medium containing 2% B27 (minus vit A), 1% GlutaMAX, and 1% penicillin-streptomycin solution (all from Invitrogen) supplemented with recombinant FGF-2 and EGF (20 ng/ml, PeproTech), as previously described (growth medium; [18]). NPCs were passaged at 70–80% confluence by harvesting with Accutase (PAA Laboratories) and re-plating at 10^4 cells/cm^2. Cell cultures were kept in a 5% CO_2 humidified atmosphere at 37 °C. All experiments with NPCs were performed using cells, obtained after 2–3 passages following thawing, grown for 48 h in medium containing 2 ng/ml FGF-2 and EGF before analysis. Cells were previously proved to be positive for the NPC markers nestin and Sox2 [35].

2.2. In vitro cell proliferation and differentiation assays

For proliferation assay, NPCs were dissociated and plated at a density of 0.5×10^5 cells/ml in growth medium into 96-well plates. Cell proliferation was determined quantifying the amount of incorporated bromodeoxyuridine (BrdU) using a labeling detection kit (Millipore) according to the manufacturer's instructions. The extent of BrdU intake was determined by immunostaining for BrdU, fixing the cells, denaturing the DNA and measuring the absorbance with a plate reader at the measure-reference wavelengths of 450–595 nm. To ensure validity of the experiment, for each time point, wells with only the culture media (no cells) and cells without BrdU labeling were included in the assay [18].

To assay neural differentiation, NPCs were plated at a density of 0.4×10^4 cells/ml in growth medium onto PDL/laminin coated 18 mm glass coverslips placed in a 12 multiwell plate. After 48 h the growth medium was replaced by neurobasal medium containing 2% B27, 1% GlutaMAX, and 1% penicillin-streptomycin solution supplemented with 5 ng/ml FGF-2. Differentiation of NPCs was performed for a total of 7 days with a progressive FGF-2 withdraw and 4 days without growth factors, replacing the medium every 2 days [35]. Neurons were recognized by immunocytochemistry essentially as reported in [35] using a rabbit anti-doublecortin (DCX) antibody (1:300; Santa-Cruz Biotech) and a secondary anti-rabbit antibody conjugated with Alexa fluor488. The cover glasses were mounted with ProLong™ Gold Antifade Mountant with 4′,6-diamidin-2-fenilindolo (DAPI) (ThermoFisher) and total nuclei and DCX-labeled cells were visualized and counted under a Leica TCS SP5 II microscope (40 X objective).

2.3. Confocal microscopy

Mitochondria were visualized in live NPCs by using laser scanning confocal microscopy imaging. Both wt and Ts65Dn NPCs were incubated for 15 min at 37 °C with 0.5 μM MitoTracker®deepRed (Molecular Probes), used as a fluorescent mitochondria-targeted marker. After washing with PBS, stained cells were examined under a Leica TCS SP5 II microscope using 63X/1.25 oil immersion objective. The red fluorescence of the MitoTracker®deepRed was analyzed by exciting the sample with a HeNe laser (excitation wavelength of 633 nm). Images were acquired using Leica Application Suite Advanced Fluorescence (LAS AF) software, version 2.2.1 (Leica Microsystems CMS GmbH) and processed using ImageJ, version 1.48.

For quantitative analysis of mitochondrial network morphology, the acquired images were conveniently adjusted for background and brightness/contrast then analyzed with MitoLoc, a plugin of ImageJ according to [36] for calculation of fragmentation index (*f* index), accounting for mitochondrial surface area and volume, and tubularity, accounting for mitochondrial network compactness [36].

2.4. Transmission electron microscopy

Ts65Dn and wt neuronal progenitor cells were collected by centrifugation. Cell pellets were washed in PBS and fixed in 2,5% glutaraldehyde for 2 h at 4 °C. Specimens were post-fixed in 0.1 M osmium tetroxide for 2 h at room temperature, dehydrated by a graded series of

ethanol and then embedded in epoxidic resin. Ultrathin sections were placed on formvar carbon grids, stained with uranyl acetate and lead citrate and analyzed under a Jeol electron microscope. Three independent samples were analyzed for each experimental condition and images from at least 10 individual cells for each sample were acquired at the same magnification. The area, the ratio between major and minor axes (aspect ratio: AR) and circularity, i.e. $4\pi \times [\text{area}/(\text{perimeter})^2]$, were recorded, by using the image J software [37], from a minimal number of 100 mitochondria sections for each sample.

2.5. Immunoblot analysis

NPCs were lysed with 0.1% Triton in PBS in the presence of a protease and phosphatase inhibitor cocktails (Sigma-Aldrich). Cell lysate (0.05 mg protein) was resolved on a 10% SDS-NuPAGE Bis/Tris gel (Life Technologies), and transferred to a polyvinylidene difluoride membrane (Millipore). Membranes were blocked in TBS-T (50 mM Tris, 150 mM NaCl, 0.01% Tween 20, pH 7.5) containing 5% BSA and probed with the following primary antibodies overnight at 4 °C: anti-Drp1 (1:500 dilution, Millipore); anti-p-S636-Drp1 (1:500 dilution, Cell Signalling); anti-RCAN1 immune-reacting with the 28-kD isoform 1 of RCAN1 (1:1000 dilution, Sigma-Aldrich,); anti-Mnf2 (1:1000 dilution, Millipore); anti-Opa1 (1:1000 dilution, Thermo Scientific). Immunoblot analysis was performed, using horseradish peroxidase-conjugated anti-mouse or anti-rabbit secondary antibodies and enhanced chemiluminescence western blotting reagents (Amersham, Pharmacia Biotech). Membranes were also probed with anti-actin antibody (1:2000 dilution, Sigma Aldrich) as internal loading control and densitometry value of immunoreactive bands for each sample was normalized versus the corresponding densitometry value of actin.

2.6. Measurement of mitochondrial ATP production rate and ATP cellular levels in NPCs

The rate of ATP production by OXPHOS was determined in digitonin-permeabilized cells, essentially, as previously described [18]. Briefly, NPCs (0.3–0.5 mg protein) were incubated at 37 °C in 2 ml of the respiratory medium pH 7.4 containing 210 mM mannitol, 70 mM sucrose, 3 mM $MgCl_2$, 20 mM Tris/HCl, 5 mM KH_2PO_4/K_2HPO_4 (pH 7.4), in the presence of the ATP detecting system consisting of glucose (2.5 mM), hexokinase (2 e.u.), glucose 6-phosphate dehydrogenase (1 e.u.) and $NADP^+$ (0.25 mM) in the presence of succinate (5 mM) plus rotenone (3 μM), as energy source, plus 10 μM diadenosine pentaphosphate, used to specifically inhibit adenylate kinase. After 5 min of incubation with digitonin (0.01% w/v), ADP (0.5 mM) was added to start the reaction and the reduction of $NADP^+$ in the extra-mitochondrial phase was monitored as an increase in absorbance at 340 nm. As a control, the ATP synthase inhibitor oligomycin (OLIGO, 5 μg/10 μl) was added in course of reaction to show the inhibition of the mitochondrial ATP production.

Cellular ATP was extracted from NPCs, previously detached from plate, using the boiling water procedure, as described in [38]. The amount of intracellular ATP was determined enzymatically in the extracts, as described in [8].

2.7. Measurement of ATPase activity

Measurements of ATPase activity was carried out in the mitochondrial membranes isolated from NPCs as described in [10].

Mitochondrial membranes were suspended in the respiratory medium pH 7.4 and ATPase was measured at 37 °C by monitoring the oligomycin (OLIGO)-sensitive ATP hydrolase activity. The biological samples (0.3 mg mitochondrial proteins) were added to 1 ml of respiratory medium (pH 7. 4) in the presence of 0.3 mM cyanide, 8 μM rotenone and 0.2 mM NADH). The addition of a freshly prepared mixture containing 5 mM $MgCl_2$, 2 mM phosphoenolpyruvate, 0.5 mM ATP, pyruvate kinase (1 e.u.) and L-lactate dehydrogenase (2 e.u.) triggers the ATP hydrolase activity, monitored as a decrease in absorbance at 340 nm, reflecting NADH oxidation, as a function of time; the reaction was inhibited by adding 5 μM OLIGO. The OLIGO-sensitive ATP hydrolase activity was measured as difference between the initial rate of NADH oxidation after the addition of the above indicated mixture and the residual rate of NADH oxidation measured after the addition of OLIGO and reported as nmol NADH oxidized/min × mg sample protein ($\varepsilon_{340nm} = 6.3\ mM^{-1}\ cm^{-1}$).

2.8. Statistical analysis

Data are reported as mean values ± standard deviation (SD). Statistical evaluation of the differential analysis between groups was performed by one-way ANOVA and Bonferroni post hoc test or Student's *t*-test as appropriate. The threshold for statistical significance was set at $P < 0.05$.

3. Results

3.1. Altered mitochondrial dynamics in Ts65Dn NPCs: shift toward mitochondrial fission

First we investigated mitochondrial network, mitochondrial ultrastructure and analyzed the levels of some proteins involved in the control of mitochondrial dynamics during NPC proliferation.

NPCs from both Ts65Dn and wt mice were stained with MitoTracker®deepRed and mitochondrial morphology imaged by confocal microscopy (Fig. 1). In wt cells mitochondria appeared elongated and mitochondrial network exhibited a branched and tubular morphology (Fig. 1A). In Ts65Dn NPCs mitochondria appeared fragmented into short rods or spheres (Fig. 1A). Confocal quantization analysis revealed in Ts65Dn cells a very significant ($P = 0.00018$) increase in the fragmentation index (Fig. 1B; *f* index = 49,95 ± 19) and a significant ($P = 0.0102$) decrease in mitochondria tubularity (Fig. 1C; tubularity index = 0.11 ± 0.015) respect to wt cells having *f* index of 20.59 ± 12 and tubularity index of 0.14 ± 0.02, thus indicating an altered mitochondrial dynamics.

To confirm the changes in mitochondrial network observed by confocal microscopy, we undertook an ultrastructural analysis by transmission electron microscopy (Fig. 2). Taking into account that we were analyzing mitochondria sections, we reasoned that in case of fragmentation we should observe a reduction in mitochondria section surface (area) and an increase in number of mitochondria sections with a roundish shape with respect to those with an elongated tubular-like shape. To evaluate this latter parameter, we measured the aspect ratio (AR), i.e. the ratio between the major and the minor axe. Mitochondrial sections with AR included between 1 and 2 were considered near to a circle shape, while those with AR above 2 approximate an ellipse. We also analyzed circularity for which a value of 1.0 indicates a perfect circle. As the value approaches 0.0, it indicates an increasingly elongated shape.

As shown in Fig. 2A, in the box plot displaying the distribution of area values in the experimental classes (Fig. 2B) and in the statistical analysis reported in Table 1, mitochondria sections of Ts65Dn cells had a significantly reduced area with respect to wt cells. Moreover, Ts65Dn cells had a lower raw AR ratio mean value and a higher raw circularity mean value with respect to wt cells (Table 1), suggesting an increase of roundish mitochondria and a decrease of elongated forms. This is clearly evident by the analysis of the percentage of mitochondria sections with a roundish shape (AR included between 1 and 2 or circularity included between 0.7 and 1) that was indeed higher in Ts65Dn than wt cells (Fig. 2C, D). No significant differences were recorded in cristae shape and organization between Ts65Dn and control cells.

To assess the molecular mechanism involved in the alteration of mitochondrial dynamics observed in NPCs, we analyzed Drp1 and

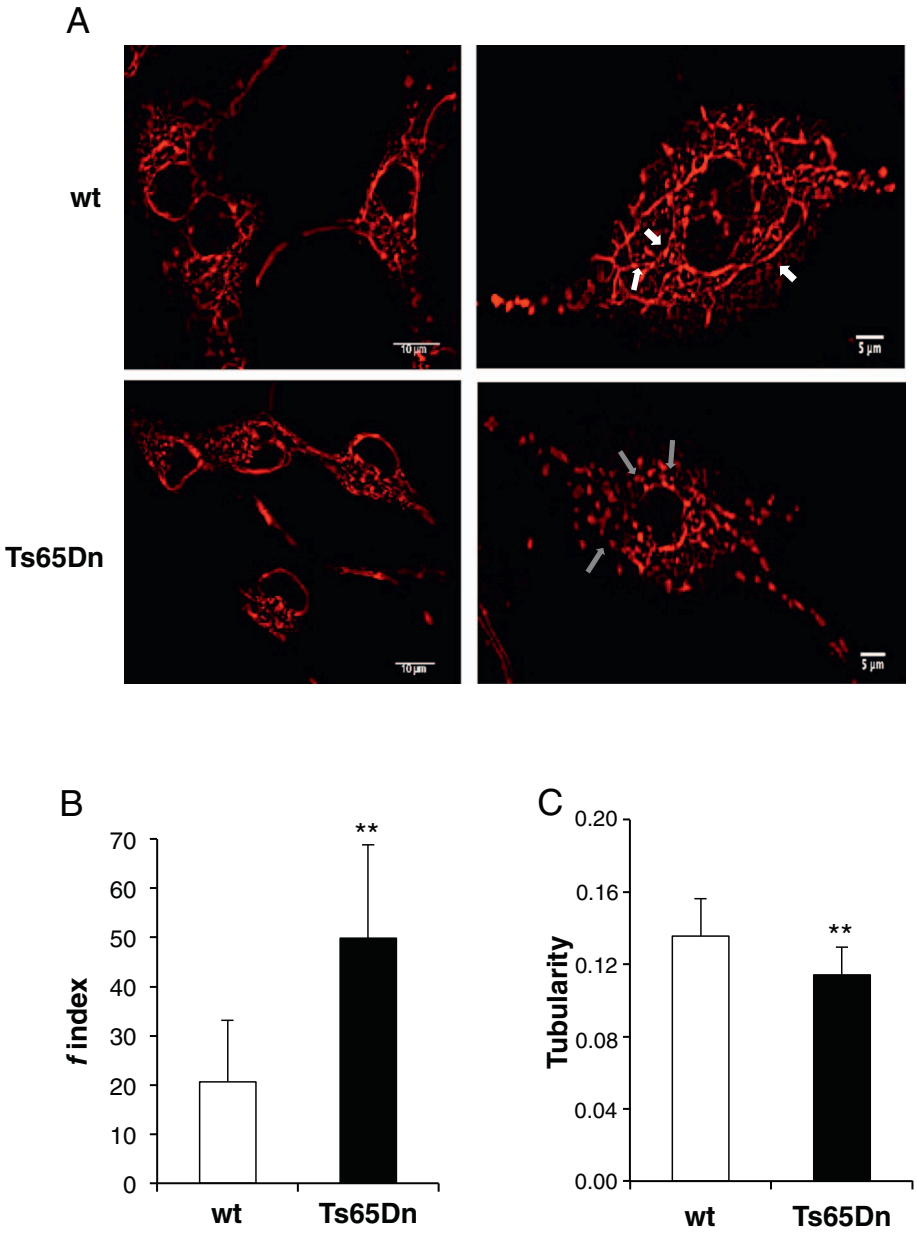

Fig. 1. Impairment of mitochondrial network in Ts65Dn-NPCs. (A) Representative images obtained by Confocal Microscopy of live cultured wt and Ts65Dn NPCs loaded with 0.5 µM MitoTracker®deepRed. White arrows indicate elongated mitochondria and grey arrows highlight spheroid mitochondria. Quantification of (B) the fragmentation index (*f* index) and (C) the compactness (tubularity) of mitochondrial networks in wild type (wt) and Ts65Dn NPCs. Data are the mean values (± SD) of the analyses performed in 27 cells for wt NPCs and 20 cells for Ts65Dn NPCs. Significant differences, calculated with Student's *t*-test, are indicated with asterisks (** = $P < 0.01$).

Mnf2, as key proteins mediating the process of mitochondrial fission and fusion, respectively. As shown by representative immunoblots and by statistical analysis of protein band densitometry, Drp1 protein level was significantly increased ($P < 0.01$) in Ts65Dn cells with respect to wild-type NPCs (Fig. 3A and B), while Mnf2 was decreased ($P < 0.05$) (Fig. 3D). The ratio between the percentage of Mfn2 and Drp1 protein levels, which accounts as an index of the balance between fusion and fission processes, was of 0.58 ± 0.09 in Ts65Dn cells, thus, shifted toward increased mitochondrial fission. In addition to Mnf2, Opa1 is another protein involved in mitochondrial fusion. Opa1 also undergoes constitutive processing leading to the conversion of the uncleaved long Opa1 (L-Opa) in cleaved short Opa1 (S-Opa). Western blotting analysis with an antibody that recognizes L-Opa and S-Opa forms revealed in Ts65Dn cells a strong decrease of L-Opa (46.82 ± 11% respect to wt) and the appearance of S-Opa form (Fig. 3E and F) which accounts for mitochondrial fragmentation [39,40].

Drp1 activity is regulated by CaN-dependent dephosphorylation at serine 637 which induces translocation of Drp1 from the cytoplasm to mitochondria where it stimulates fission [41,42]. Because RCAN1 overexpression in DS might alter Drp1 dephosphorylation, we analyzed protein levels of RCAN1 and phosphorylation of Drp1 at S637 (P-Drp1) in Ts65Dn NPCs compared to wt cells. Immunoblotting analysis (Fig. 3A and B) showed an increase of RCAN1 protein levels ($P < 0.01$) and a great reduction of P-Drp1 in NPCs from Tn65Dn mice ($P < 0.01$) with respect to wt cells. The densitometry analysis of immunodetected bands shows the decrease of the ratio between P-Drp1 and Drp1 protein levels (0.48 ± 0.14; Fig. 3C), suggesting an increase of dephosphorylated form of Drp1 in NPCs.

3.2. Mdivi-1 treatment of Ts65Dn NPCs reverses alteration of mitochondrial network

To test the role of Drp1 in alteration of mitochondrial dynamics and function in Ts65Dn NPCs, we made use of Mdivi-1, a specific inhibitor of Drp1 assembly and translocation into mitochondria and therefore of mitochondrial fission [29,43].

Mdivi-1 concentration of 10 µM, showing no toxic effect in cultured neurons, was chosen according to Liu and colleagues [44]. Ts65Dn

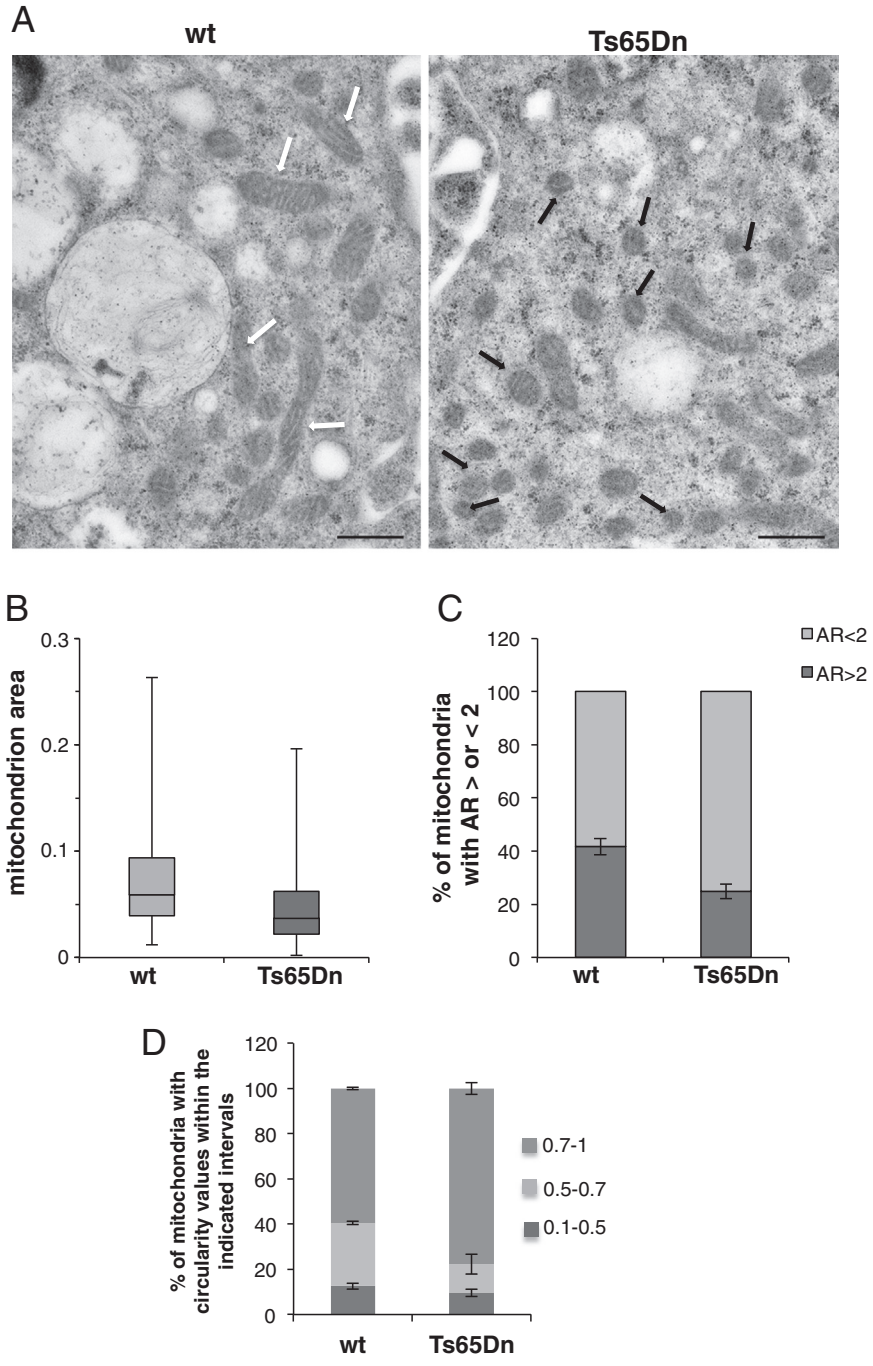

Fig. 2. Ultrastructure analysis reveals mitochondria fragmentation in Ts65Dn-NPCs. (A) Representative images of mitochondria visualized by transmission electron microscopy in a wt and Ts65Dn cell. Scale bars correspond to 0.6 μm. White arrows indicate representative elongated mitochondria and black arrows highlight representative spheroid mitochondria. (B) Box plot shows the distribution of mitochondria section area in Ts65Dn and wt cells; horizontal lines in the box plot indicate the mean values. (C) Histogram depicts the percentage of mitochondria with AR values > of 2 (i.e. elongated) and < 2 (i.e. near a roundish shape) in Ts65Dn and control cells. (D) Histogram depicts the percentage of mitochondria with circularity values included in the intervals 0.1–0.5; 0.5–0.7; 0.7–1 (a perfect circle shows a circularity value of 1). Data result from the analysis of a minimal number of 100 mitochondria sections from at least 10 individual cells from three independent samples for each NPC genotype (wt and Ts65Dn). For significant differences and statistical analysis please refer to Table 1.

cultured NPCs were incubated either with Mdivi-1 or the same volume of vehicle (DMSO), for 24 h.

As first, we checked whether Mdivi-1 could affect Drp1 expression and phosphorylation. As expected, and according to [29,43], no significant differences were found in Drp1 and P-Drp1 protein levels between untreated and Mdivi-1-treated Ts65Dn NPCs (Fig. 4A), indicating that Mdivi-1 treatment had no effect on both expression and phosphorylation status of Drp1 in NPCs.

The effect of Mdivi-1 on mitochondrial network and morphology of Ts65Dn NPCs were then analyzed by confocal and transmission electron microscopy.

Confocal microscopy analysis revealed that following treatment with Mdivi-1 the mitochondria of Ts65Dn cells acquired the typical tubular morphology (Fig. 4B) already observed in wild-type cells (see Fig. 1A). Confocal quantization analysis revealed in Mdivi-1-treated Ts65Dn cells both a significant ($P = 0.0078$) decreased fragmentation (Fig. 4C; f index = 37 ± 2.96) and a very strong ($P = 0.0001$) increase in mitochondria tubularity (Fig. 4D; tubularity index = 0.22 ± 0.02) with respect to untreated Ts65Dn neural progenitor cells, having a f index of 50.2 ± 3.48 and a tubularity index of 0.12 ± 0.01.

To give more information of Mdivi-1 effect on mitochondrial morphology and dimensions, ultrastructural analysis was performed in Mdivi-1-treated Ts65Dn cells. Mitochondrial area and the percentage of mitochondria sections with AR > 2 were notably increased following Mdiv-1 treatment while mitochondria with a circularity value > 0.7 decreased (Fig. 5 and Table 1), which restores a wt-like condition of mitochondrial area and structure (see also Fig. 2A and Table 1).

Altogether, these results showed that inhibition of mitochondrial fission by Mdivi-1 resulted in an improvement of mitochondrial

Table 1
Data from the ultrastructural analysis performed on mitochondria from wild-type and Ts65Dn NPCs or on mitochondria from Ts65Dn NPCs treated either with 10 μM Mdivi-1 (Ts65Dn NPCs + Mdiv-1) or DMSO (Ts65Dn NPCs + vehicle).

		Wild-type NPCs	Ts65Dn NPCs	Ts65Dn NPCs + vehicle	Ts65Dn NPCs + Mdivi-1
Area	Mean surface area (square pixels)	0.076	0.050	0.048	0.069
	SD between single values for cell type	0.0552	0.043	0.0378	0.0486
	SD between mean values of independent samples	0.0005	0.0048	0.0044	0.0122
	P value between mean values of single samples from each cell type		**0.048**		**0.05**
	P value between all recorded values for cell type		**1.21E-09**		**2.30E-09**
AR	Mean area ratio values	2.06	1.85	1.77	1.95
	SD between single values for cell type	0.9246	0.9909	0.8925	0.9216
	SD between mean values of independent samples	0.058	0.027	0.003	0.1
	P value between mean values of single samples from each cell type		0.06		0.08
	P value between all recorded values for cell type		**0.01**		**0.01**
Circularity	Mean circularity values	0.73	0.79	0.81	0.76
	SD between single values for cell type	0.1782	0.1692	0.1490	0.1602
	SD between mean values of independent samples	0.0039	0.0019	0.0032	0.0258
	P value between mean values of single samples from each cell type		0.01		0.08
	P value between all recorded values for cell type		**7.92E-05**		**0.01**

Cells were processed as described in the legends of Figs. 2 and 5. Mitochondrial area (expressed in square pixels), AR (the ratio between major and minor axe) and the circularity ($4\pi \times [\text{area}/(\text{perimeter})^2]$) were recorded for each mitochondrion section by using the image J software. Statistical analysis was performed by Student's *t*-test analysis evaluated as follow: i) the *P* value between all recorded values for cell type is calculated considering the single values of all mitochondrial section recorded in wt NPCs vs Ts65Dn NPCs or Ts65Dn NPCs + vehicle vs Ts65Dn NPCs + Mdivi-1; ii) the *P* value between all recorded values for cell type is calculated considering the mean values of the three independent experiments in wt NPCs vs Ts65Dn NPCs or Ts65Dn NPCs + vehicle vs Ts65Dn NPCs + Mdivi-1. Statistically significant values are indicated in bold.

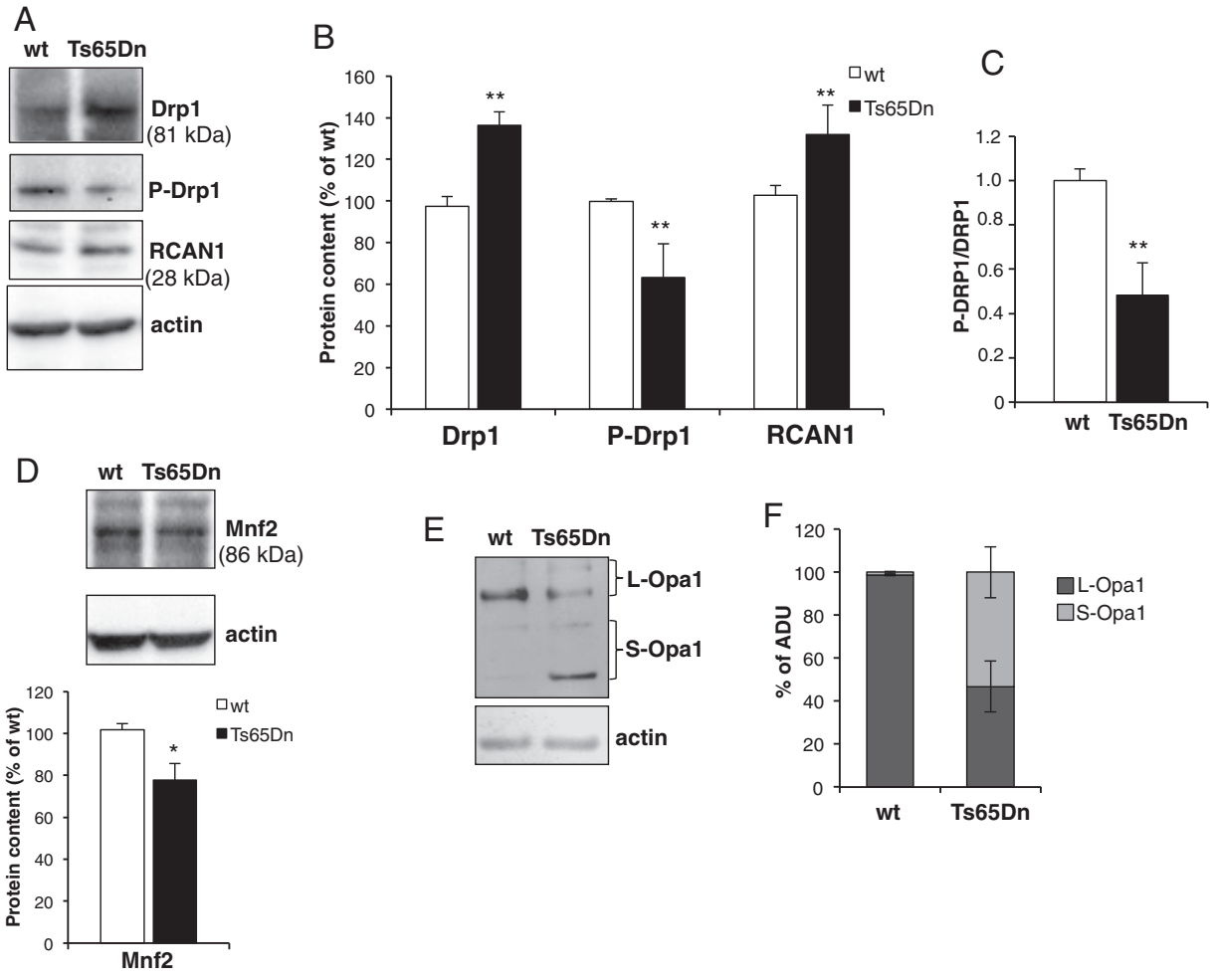

Fig. 3. Levels of proteins involved in the mitochondrial fission and fusion process.(A) Representative immunoblot and (B) densitomentric analysis of Drp1, Drp1 phosphorylation at S637 (P-DRP1) and RCAN1 protein levels measured in cell extracts (0.05 mg protein) of wt and Ts65Dn NPCs. (C) Histrogram shows the ratio between P-Drp1 and Drp1. (D) Representative immunoblot and densitomentric analysis of Mnf2 protein levels measured in cell extracts (0.05 mg protein) of wt and Ts65Dn NPCs. (E) Representative immunoblot of long (L-Opa1) and short (S-Opa1) forms of Opa1 proteins measured in cell extracts (0.05 mg protein) of wt and Ts65Dn NPCs. (F) The histogram represents the percentage of arbitrary densitometric unit (ADU) of L and S forms of Opa1 in each lane. Data are mean values (± SD) of two independent measurements carried out in three independent samples for each NPC genotypes (wt and Ts65Dn) and expressed as percentage of wt. Significant differences, calculated with Student's *t*-test, are indicated with asterisks (** = $P < 0.01$; * = $P < 0.05$).

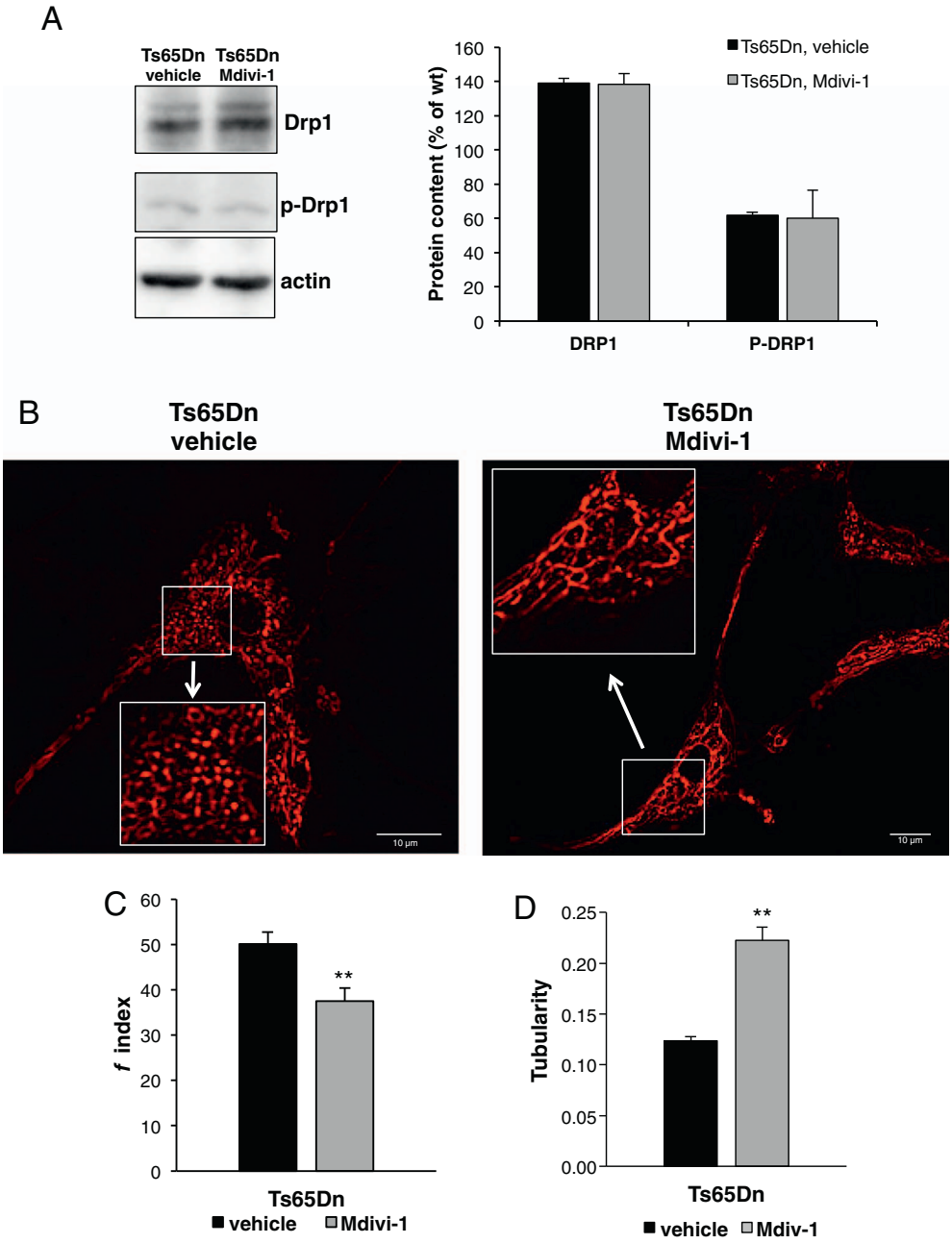

Fig. 4. Mdivi-1 has no effect on Drp1 protein expression and phosphorylation but improves mitochondrial network organization. Ts65Dn NPCs were incubated either with 10 µM Mdivi-1 (Ts65Dn Mdivi-1) or vehicle (0.05% DMSO) (Ts65Dn vehicle) for 24 h. (A) Representative immunoblot and (B) densitomentric analysis of Drp1 and Drp1 phosphorylation at S637 (P-Drp1) protein levels measured in cell extracts (0.05 mg protein) of NPCs treated and untreated Ts65Dn cells. Data are mean values (± SD) of three independent experiments and expressed as percentage of wt. Differences between Ts65Dn vehicle and Ts65Dn NPCs treated with Mdivi-1 are not significant ($P > 0.05$). (B) Representative images obtained by confocal microscopy of cultured Ts65Dn NPCs treated with Mdivi-1 or vehicle loaded with 0.5 µM MitoTracker®deepRed. The panel inside shows a higher magnification of the image in the white box. (C) Quantification of the fragmentation index (*f* index) and (D) the tubularity of mitochondrial networks in untreated and Mdivi-1-treated Ts65Dn NPCs. Data are the mean values (± SD) of the analyses performed in 20 Ts65Dn cells plus vehicle and 27 Ts65Dn cells plus Mdivi-1. Significant differences, calculated with Student's *t*-test, are indicated with asterisks (** = $P < 0.01$).

network organization in Ts65Dn cells.

3.3. *Mdivi-1 treatment counteracts mitochondrial dysfunctions, restores cell energy deficit and enhances in vitro neurogenesis of Ts65Dn NPCs*

To test whether inhibition of mitochondrial fission by Mdivi-1 could counteract the deficit of OXPHOS capacity found in Ts65Dn NPCs [18], we measured mitochondrial ATP production and ATPase activity in cultured NPCs in the presence of 10 µM Mdivi-1 or vehicle (DMSO), for 24 h.

As shown in Fig. 6, exposure of Ts65Dn cells to Mdivi-1 prevented both the impairment of mitochondrial ATP production via OXPHOS (Fig. 6A) and the deficit of ATPase activity in Ts65Dn cells (Fig. 6B).

Consequently, measurement of the cellular ATP levels demonstrated that Mdivi-1 treatment significantly prevents the strong reduction of cellular ATP pool (64.8% ± 5 respect to wt, $P < 0.01$) and confers to Ts65Dn cells the capability to maintain the cellular ATP content comparable to that of wt cells (Fig. 6C).

Next, we investigated whether improvement of mitochondrial dynamics and bioenergetics could affect Ts65Dn cell proliferation and differentiation, a measure of neurogenesis *in vitro* [45]. We first determined NPC proliferative capacity in untreated and Mdivi-1-treated Ts65Dn cells by BrdU incorporation experiments. As shown in Fig. 6D, Ts65Dn NPCs showed about 40% reduction of proliferation as compared to wt cultures. Mdivi-1 treatment significantly promotes proliferation capacity in Ts65Dn NPCs, making them able to divide at the same level of wt cells. We next evaluated the Mivi-1 effect on Ts65Dn NPC differentiation. A statistically significant increase in DCX-positive NPCs, a marker for newly generated hippocampal neurons [46], was found in the presence of 10 µM Mdivi-1 under differentiation condition (Fig. 6F; 13% ± 5 and 28% ± 7 DCX-positive neurons in untreated and Mdivi-1-treated Ts65Dn cells, respectively; $P < 0.01$). Overall, these data indicated enhanced proliferation and differentiation of Ts65Dn hippocampal cells following Mdivi-1 treatment.

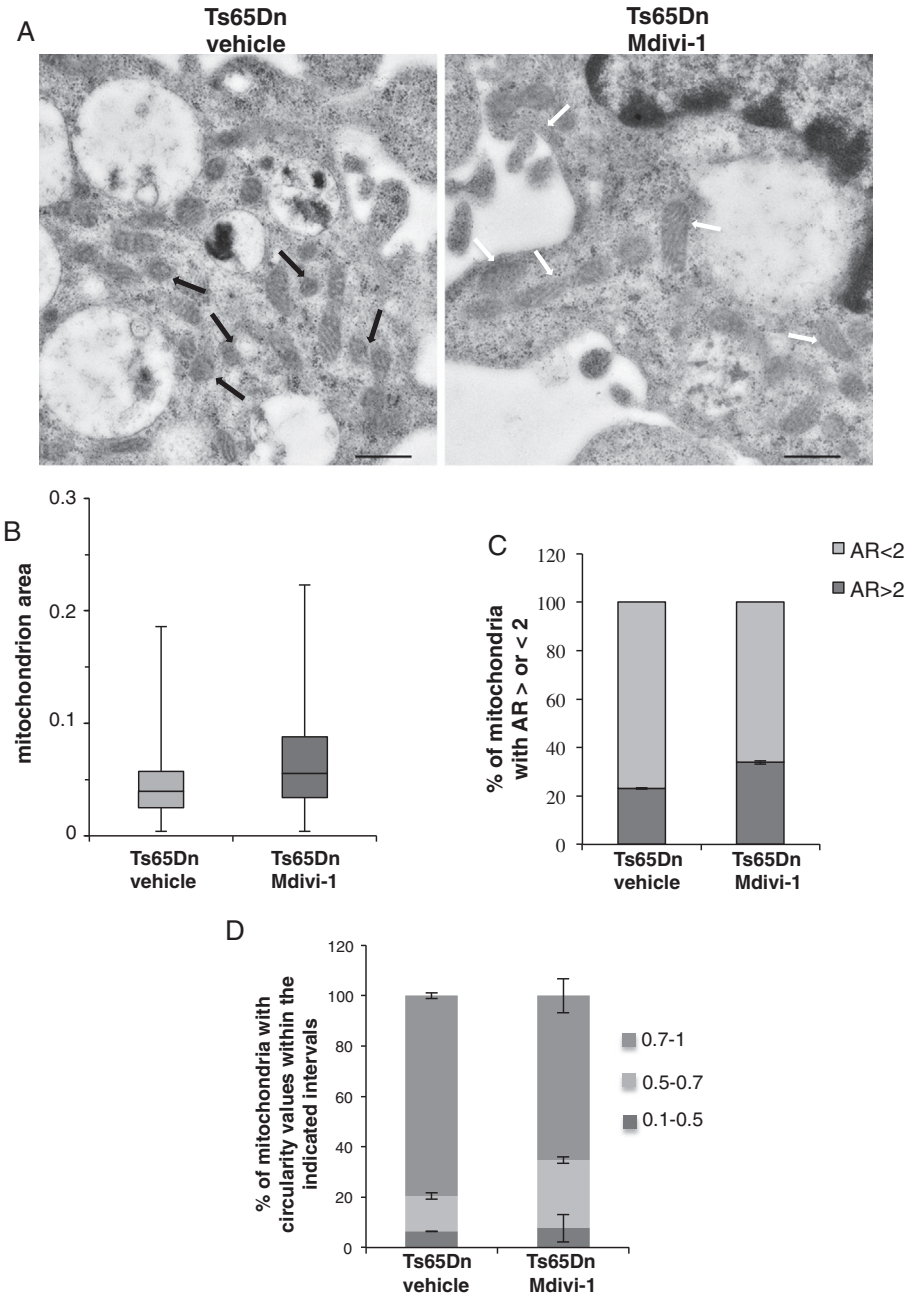

Fig. 5. Mdivi-1 inhibits mitochondrial fragmentation. Ts65Dn NPCs were incubated either with 10 μM Mdivi-1 (Ts65Dn Mdivi-1) or vehicle (0.02% DMSO) (Ts65Dn vehicle) for 24 h and fixed with glutaraldehyde and manipulated as described in Material and Methods (A) Representative images of mitochondria visualized by Trasmission Electron Microscopy. Scale bars correspond to 0.6 μm. Black arrows indicate representative spheroid mitochondria, white arrows representative elongated mitochondria. (B) Box plot shows the distribution of mitochondria section area in untreated or Mdiv-1-treated Ts65Dn cells; horizontal lines in the box plot indicate the mean values. (C) Histogram depicts the percentage of mitochondria with AR values > of 2 (i.e. elongated) and < 2 (i.e. near a roundish shape) in untreated or Mdiv-1-treated Ts65Dn NPCs. (D) Histogram depicts the percentage of mitochondria with circularity values included in the intervals 0.1–0.5; 0.5–0.7; 0.7–1 (a perfect circle shows a circularity value of 1). Data result from the analysis of a minimal number of 100 mitochondria sections from at least 10 individual cells for each sample in three independent experiments. For significant differences and statistical analysis please refer to Table 1.

4. Discussion

In this study we provide evidence that an increase of Drp1-dependent mitochondria fission occurs during the proliferation of cultured adult hippocampal progenitors from Ts65Dn mouse model of DS. In these cells, mitochondrial fission is associated with an increase in protein level and dephosphorylation of Drp1, a decrease of Mnf2 and a conversion of L-Opa1 into S-Opa1. Interestingly, the treatment of these cells with Mdivi-1, an inhibitor of Drp1, decreases mitochondrial fission, restores mitochondrial network, prevents mitochondrial dysfunctions and stimulates NPC proliferation and neural differentiation. Our results provide new insight on the origin of mitochondrial dysfunction in DS, shed light on how mitochondrial dysfunctions could contribute to impaired adult neurogenesis in DS, and pave the way for the use of new therapeutic drugs in managing some energy deficit-associated DS clinical manifestations.

Neurons critically depend on mitochondrial structural network organization and bioenergetics to execute the complex processes of neurogenesis, neurotransmission and synaptic plasticity [4,5,47,48]. Indeed, alteration of mitochondrial dynamics strongly affects neuronal progenitor proliferation and neuronal function, survival and differentiation in several models of neurodegenerative diseases (for refs see [49]). Mitochondrial morphology, size and position within cells are maintained through a balance of fission and fusion events. Perturbation of the steady state between these opposing processes has been directly implicated in several human disorders [50].

A reduction in fusion process has been recently described in peripheral DS fibroblasts [15]. Consistently, we found in NPCs from Ts65Dn mice a reduction in mitochondrial fusion due to the down-regulation of Mnf2 protein level and, increased processing of Opa1 into short Opa1 form, both known to be involved in promoting mitochondrial fragmentation [39,40]. Given that PGC-1α has been reported to promote the expression of the Mnf2 [15,51], the reduced protein levels of Mnf2 in Ts65Dn NPCs may be linked to the PGC-1α down-regulation

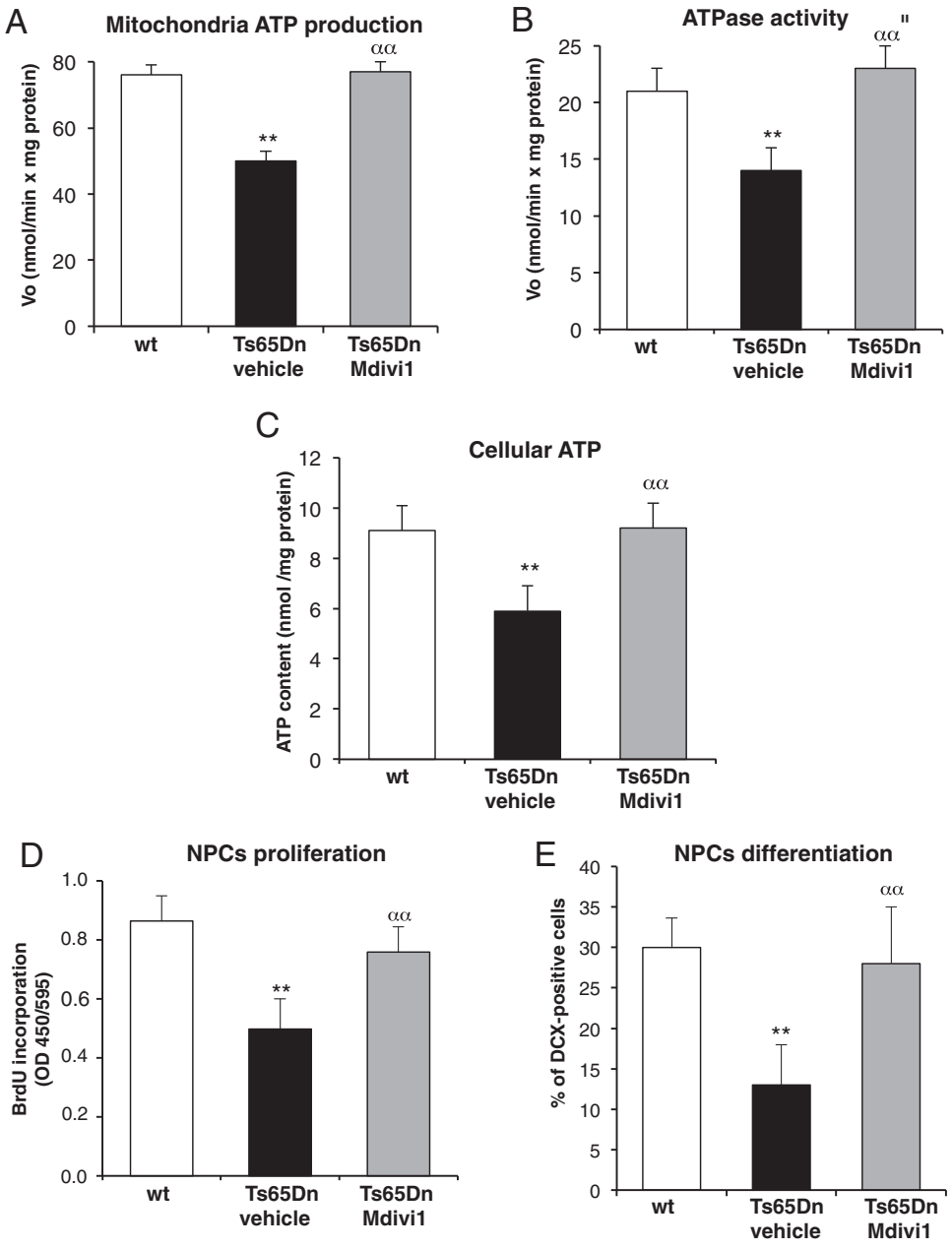

Fig. 6. Mdivi-1 rescues the deficit of mitochondrial bioenergetics and enhances proliferation and neural differentiation of Ts65Dn NPCs. Ts65Dn NPCs were incubated either with 10 μM Mdivi-1 (Ts65Dn Mdivi-1) or vehicle (0.05% DMSO) (Ts65Dn vehicle) for 24 h. wt NPCs were also used as control (wt). (A) The rate of mitochondrial ATP production via OXPHOS was measured spectrophotometrically in 0.3 mg of protein in the presence of the respiratory substrate succinate (5 mM), as described in Material and Methods. ATP production was expressed as nmol/min × mg protein. (B) The ATPase activity was measured spectrophotometrically in mitochondrial membrane enriched fractions (0.3 mg protein) as described under Materials and Methods and expressed as nmol/min × mg protein. (C) ATP cellular content was measured fluorimetrically in cell extract as described under Materials and Methods and expressed as nmol/min × mg protein. (D) NPC proliferation was analyzed by BrdU incorporation. Data are represented as relative levels of BrdU incorporation in wt and untreated (vehicle) and treated (Mdivi-1) Ts65Dn NPCs. Results are mean values of optic density (OD) at the measure-reference wavelengths of 450–595 nm obtained from ELISA assay experiments. (E) Ts65Dn NPCs were treated with Mdivi-1 or vehicle under differentiation conditions (see Materials and Methods). Expression of DCX indicates neuronal differentiation.
Data in each panel represent the mean value (± SD) of at least three independent experiments and significant differences, calculated with one-way ANOVA and Bonferroni test, are indicated as follow: wt NPCs vs Ts65Dn NPCs, ** = $P < 0.01$; Ts65Dn NPCs vs Ts65Dn NPCs treated with Mdivi-1, αα = $P < 0.01$.

that we previously demonstrated in these cells [18].

In neuronal progenitor cells from trisomic Ts65Dn mice we also found a shift of the balance fission/fusion toward a higher fission with an up-regulation of Drp1 expression and activity. Imbalance of the only Drp1 protein is sufficient to produce excessive fission that leads to mitochondrial dysfunction [52]. For the fission event, Drp1 translocates from the cytoplasm to mitochondria where it forms an oligomeric structure that induces fragmentation of mitochondrial membranes [53]. We confirmed a high fission process in Ts65Dn NPCs by both ultrastructural evaluation of mitochondrial area and shape, as well as by mitochondrial network visualization by confocal microscopy. Our data are in agreement with recent studies showing that an up-regulation of Drp1-mediated mitochondrial fission is commonly observed in various neurological disorders (for refs see [54]) together with a decrease in calcineurin-dependent dephosphorylation of Drp1 at S637, which regulates Drp1 translocation from cytoplasm to mitochondria [41,42]. Our results, showing an up-regulation of Drp1 protein content and a decrease of S637 phosphorylation, could account for higher translocation of Drp1 from cytosol to mitochondria in Ts65Dn NPCs with respect to wt cells, thus providing further explanation for the alteration in shape and network. It is known that PKA-dependent phosphorylation of S637 exerts the opposing effect, i.e. maintains Drp1 in the cytosol and inhibits fission [55]. Thus, it could be that calcineurin-mediated dephosphorylation of Drp1 prevails over PKA-dependent phosphorylation. This is consistent with the finding that a down-regulation of PKA activity and cAMP signalling occurs in hippocampus of Ts65Dn mice [56] and DS cells [9]. Interestingly, we confirmed that, as previously reported [28], the chromosome 21 gene RCAN1, the regulator of calcineurin 1, is overexpressed in Ts65Dn cells. This suggests that RCAN1 overexpression in DS could account for Drp1 up-regulation and the consequent increase in mitochondrial fission.

It has been reported that shifting the balance of mitochondrial morphology toward fission enhances susceptibility to mitochondrial dysfunctions, oxidative stress and cell death; conversely, fused mitochondria are energetically more active, preserve cell functions, and can better tolerate oxidative stress [57]. Recently, Khacho and co-

workers [58] have also demonstrated that increased mitochondrial fission is associated with defective neural stem cell proliferation and that mitochondrial dynamics is an upstream regulator of essential mechanisms governing neural stem cell self-renewal and differentiation.

Given the involvement of Drp1 in mitochondrial fission, and the defective hippocampal neurogenesis showed in Ts65Dn NPCs [16,17], we hypothesized that blocking Drp1 and the Drp1-dependent excessive fission, might, by one hand, give new information on the importance of mitochondrial dynamics in the regulation of adult neurogenesis in DS and, by the other, represent a new attractive strategy to correct DS-associated clinical phenotypes linked to energy deficit and defective neurogenesis. The effects of Mdivi-1 on the excessive fragmentation of mitochondria, the bioenergetics impairment and the altered neurogenesis, have proved, at least in part, our hypothesis. Mdivi-1 is a small molecule derivative of quinazolinone, which acts mainly as a selective inhibitor of the mitochondrial fission protein Drp1 through blocking Drp1 self-assembly and GTP hydrolysis [43]. Indeed, we found that Mdivi-1-dependent restoring of mitochondrial network organization counteracts mitochondrial bioenergetics impairment and, strikingly, promotes both in vitro proliferation and differentiation of hippocampal neural precursor cells. Our results are consistent with several other studies in which it has been demonstrated that mitochondrial fission is required for hippocampal neuronal proliferation and differentiation [58,59] and that Mdivi-1, by blocking the mitochondrial fission, exerts neuroprotective effects in animal models of various neurodegenerative disorders [30,32,60–62].

In conclusion, the present study provides new information on the molecular mechanisms responsible for energy deficit and altered mitochondrial bioenergetics and dynamics in DS. Moreover it demonstrates that alteration of mitochondrial network is closely linked to the impaired mitochondrial bioenergetics and *in vitro* hippocampal neurogenesis. Our conclusion is consistent with a recent study by Izzo and coworkers [15] showing mitochondrial fragmentation in DS human fetal fibroblasts and the potential of metformin, a drugs able to target mitochondria [5] and to promote mouse adult neurogenesis and spatial memory formation [63], in counteracting both mitochondrial fragmentation and dysfunctions. The specific inhibition of Drp1-dependent mitochondrial fragmentation by Mdivi-1 and the consequent effect on hippocampal neural progenitor cell proliferation and differentiation, provide a further evidence of the biological role of mitochondria in neurogenesis and bring insights on how the promotion of mitochondrial dynamics can contribute to the therapeutic treatment of Down syndrome.

Transparency document

The http://dx.doi.org/10.1016/j.bbadis.2017.09.014 associated with this article can be found, in online version.

Acknowledgment

This study was partially supported by a grant from Fondation Jerome Lejeune (VACCA/1093-VR2012B). We are particularly grateful to people that very kindly contributed to support in part this research by individual donations, in particular to “Associazione Progetto 21-Onlus” and “A.M.A.R. Down-Onlus”. We thank Dr. Andrea Contestabile for the kind gift of the cellular lines used in this study.

Disclosure

None of the authors declares financial interests or potential conflict of interests.

References

[1] S.E. Antonarakis, Down syndrome and the complexity of genome dosage imbalance, Nat. Rev. Genet. 18 (2017) 147–163.
[2] M. Kazemi, M. Salehi, M. Kheirollahi, Down syndrome: current status, challenges and future perspectives, Int. J. Mol. Cell. Med. 5 (2016) 125–133.
[3] E. Head, I.T. Lott, D.M. Wilcock, C.A. Lemere, Aging in Down syndrome and the development of Alzheimer's disease neuropathology, Curr. Alzheimer Res. 13 (2016) 18–29.
[4] D. Valenti, L. de Bari, B. De Filippis, A. Henrion-Caude, R.A. Vacca, Mitochondrial dysfunction as a central actor in intellectual disability-related diseases: an overview of Down syndrome, autism, Fragile X and Rett syndrome, Neurosci. Biobehav. Rev. 2 (2014) 202–217.
[5] D. Valenti, N. Braidy, D. De Rasmo, A. Signorile, L. Rossi, A.G. Atanasov, M. Volpicella, A. Henrion-Caude, S.M. Nabavi, R.A. Vacca, Mitochondria as pharmacological targets in Down syndrome, Free Radic. Biol. Med. (2017), http://dx.doi.org/10.1016/j.freeradbiomed.2017.08.01.
[6] B. De Filippis, D. Valenti, L. de Bari, D. De Rasmo, M. Musto, A. Fabbri, L. Ricceri, C. Fiorentini, G. Laviola, R.A. Vacca, Mitochondrial free radical overproduction due to respiratory chain impairment in the brain of a mouse model of Rett syndrome: protective effect of CNF1, Free Radic. Biol. Med. 83 (2015) 167–177.
[7] M. Golpich, E. Amini, Z. Mohamed, R. Azman Ali, N. Mohamed Ibrahim, A. Ahmadiani, Mitochondrial dysfunction and biogenesis in neurodegenerative diseases: pathogenesis and treatment, CNS Neurosci. Ther. 23 (2017) 5–22.
[8] D. Valenti, A. Tullo, M.F. Caratozzolo, R.S. Merafina, P. Scartezzini, E. Marra, R.A. Vacca, Impairment of F1F0-ATPase, adenine nucleotide translocator and adenylate kinase causes mitochondrial energy deficit in human skin fibroblasts with chromosome 21 trisomy, Biochem. J. 431 (2010) 299–310.
[9] D. Valenti, G.A. Manente, L. Moro, E. Marra, R.A. Vacca, Deficit of complex I activity in human skin fibroblasts with chromosome 21 trisomy and overproduction of reactive oxygen species by mitochondria: involvement of the cAMP/PKA signalling pathway, Biochem. J. 435 (2011) 679–688.
[10] D. Valenti, De D. Rasmo, A. Signorile, L. Rossi, L. de Bari, I. Scala, B. Granese, S. Papa, R.A., Vacca, epigallocatechin-3-gallate prevents oxidative phosphorylation deficit and promotes mitochondrial biogenesis in human cells from subjects with Down's syndrome, Biochim. Biophys. Acta 1832 (2013) 542–552.
[11] R.A. Vacca, D. Valenti, Green tea EGCG plus fish oil omega-3 dietary supplements rescue mitochondrial dysfunctions and are safe in a Down's syndrome child, Clin. Nutr. 34 (2015) 783–784.
[12] C. Piccoli, A. Izzo, R. Scrima, F. Bonfiglio, R. Manco, R. Negri, G. Quarato, O. Cela, M. Ripoli, M. Prisco, F. Gentile, G. Calì, P. Pinton, A. Conti, L. Nitsch, N. Capitanio, Chronic pro-oxidative state and mitochondrial dysfunctions are more prounounced in fibroblasts from Down syndrome foeti with congenital heart defects, Hum. Mol. Genet. 22 (2013) 1218–1232.
[13] E.A. Shukkur, A. Shimohata, T. Akagi, W. Yu, M. Yamaguchi, M. Murayama, D. Chui, T. Takeuchi, K. Amano, K.H. Subramhanya, T. Hashikawa, H. Sago, C.J. Epstein, A. Takashima, K. Yamakawa, Mitochondrial dysfunction and tau hyperphosphorylation in Ts1Cje, a mouse model for Down syndrome, Hum. Mol. Genet. 15 (2006) 2752–2762.
[14] J. Busciglio, A. Pelsman, C. Wong, G. Pigino, M. Yuan, H. Mori, B.A. Yankner, Altered metabolism of the amyloid beta precursor protein is associated with mitochondrial dysfunction in Down's syndrome, Neuron 33 (2002) 677–688.
[15] A. Izzo, M. Nitti, N. Mollo, S. Paladino, C. Procaccini, D. Faicchia, G. Calì, R. Genesio, F. Bonfiglio, R. Cicatiello, E. Polishchuk, R. Polishchuk, P. Pinton, G. Matarese, A. Conti, L. Nitsch, Metformin restores the mitochondrial network and reverses mitochondrial dysfunction in Down syndrome cells, Hum. Mol. Genet. 26 (2017) 1056–1069.
[16] R.H. Reeves, N.G. Irving, T.H. Moran, A. Wohn, C. Kitt, S.S. Sisodia, C. Schmidt, R.T. Bronson, M.T. Davisson, A mouse model for Down syndrome exhibits learning and behavior deficits, Nat. Genet. 11 (1995) 177–184.
[17] A. Contestabile, B. Greco, D. Ghezzi, V. Tucci, F. Benfenati, L. Gasparini, Lithium rescues synaptic plasticity and memory in Down syndrome mice, J. Clin. Invest. 123 (2013) 348–361.
[18] D. Valenti, L. de Bari, D. de Rasmo, A. Signorile, A. Henrion-Caude, A. Contestabile, R.A. Vacca, The polyphenols resveratrol and epigallocatechin-3-gallate restore the severe impairment of mitochondria in hippocampal progenitor cells from a Down syndrome mouse model, Biochim. Biophys. Acta 1862 (2016) 1093–1104.
[19] R.A. Vacca, D. Valenti, S. Caccamese, M. Daglia, N. Braidy, S.M. Nabavi, Plant polyphenols as natural drugs for the management of Down syndrome and related disorders, Neurosci. Biobehav. Rev. 71 (2016) 865–877.
[20] G. Benard, N. Bellance, D. James, P. Parrone, H. Fernandez, T. Letellier, R. Rossignol, Mitochondrial bioenergetics and structural network organization, J. Cell Sci. 120 (2007) 838–848.
[21] P. Mishra, D.C. Chan, Metabolic regulation of mitochondrial dynamics, J. Cell Biol. 212 (2016) 379–387.
[22] N. Birsa, R. Norkett, N. Higgs, G. Lopez-Domenech, J.T. Kittler, Mitochondrial trafficking in neurons and the role of the Miro family of GTPase proteins, Biochem. Soc. Trans. 41 (2013) 1525–1531.
[23] S.B. Berman, F.J. Pineda, J.M. Hardwick, Mitochondrial fission and fusion dynamics: the long and short of it, Cell Death Differ. 15 (2008) 1147–1152.
[24] H. Lee, Y. Yoon, Mitochondrial fission and fusion, Biochem. Soc. Trans. 44 (2016) 1725–1735.
[25] A.M. Bertholet, T. Delerue, A.M. Millet, M.F. Moulis, C. David, M. Daloyau, L. Arnauné-Pelloquin, N. Davezac, V. Mils, M.C. Miquel, M. Rojo, P. Belenguer, Mitochondrial fusion/fission dynamics in neurodegeneration and neuronal plasticity, Neurobiol. Dis. 90 (2016) 3–19.
[26] H. Wong, J. Levenga, P. Cain, B. Rothermel, E. Klann, C. Hoeffer, RCAN1 overexpression promotes age-dependent mitochondrial dysregulation related to neurodegeneration in Alzheimer's disease, Acta Neuropathol. 130 (2015) 829–843.

[27] A. Patel, N. Yamashita, M. Ascaño, D. Bodmer, E. Boehm, C. Bodkin-Clarke, Y.K. Ryu, R. Kuruvilla, RCAN1 links impaired neurotrophin trafficking to aberrant development of the sympathetic nervous system in Down syndrome, Nat. Commun. 6 (2015) 10119.
[28] M. Rachidi, C. Lopes, Mental retardation and associated neurological dysfunctions in Down syndrome: a consequence of dysregulation in critical chromosome 21 genes and associated molecular pathways, Eur. J. Paediatr. Neurol. 12 (2008) 168–182.
[29] L.L. Lackner, J. Nunnari, Small molecule inhibitors of mitochondrial division: tools that translate basic biological research into medicine, Chem. Biol. 17 (2010) 578–583.
[30] Q. Wu, S.X. Xia, Q.Q. Li, Y. Gao, X. Shen, L. Ma, M.Y. Zhang, T. Wang, Y.S. Li, Z.F. Wang, C.L. Luo, L.Y. Tao, Mitochondrial division inhibitor 1 (Mdivi-1) offers neuroprotection through diminishing cell death and improving functional outcome in a mouse model of traumatic brain injury, Brain Res. 1630 (2016) 134–143.
[31] Y. Li, P. Wang, J. Wei, R. Fan, Y. Zuo, M. Shi, H. Wu, M. Zhou, J. Lin, M. Wu, X. Fang, Z. Huang, Inhibition of Drp1 by Mdivi-1 attenuates cerebral ischemic injury via inhibition of the mitochondria-dependent apoptotic pathway after cardiac arrest, Neuroscience 311 (2015) 67–74.
[32] N. Zhang, S. Wang, Y. Li, L. Che, Q. Zhao, A selective inhibitor of Drp1, mdivi-1, acts against cerebral ischemia/reperfusion injury via an anti-apoptotic pathway in rats, Neurosci. Lett. 535 (2013) 104–109.
[33] S. Agarwal, A. Yadav, S.K. Tiwari, B. Seth, L.K. Chauhan, P. Khare, R.S. Ray, R.K. Chaturvedi, Dynamin-related protein 1 inhibition mitigates bisphenol A-mediated alterations in mitochondrial dynamics and neural stem cell proliferation and differentiation, J. Biol. Chem. 291 (2016) 15923–15939.
[34] T.D. Fischer, M.J. Hylin, J. Zhao, A.N. Moore, M.N. Waxham, P.K. Dash, Altered mitochondrial dynamics and TBI pathophysiology, Front. Syst. Neurosci. 10 (2016) 29.
[35] H. Babu, J.H. Claasen, S. Kannan, A.E. Rünker, T. Palmer, G. Kempermann, A protocol for isolation and enriched monolayer cultivation of neural precursor cells from mouse dentate gyrus, Front. Neurosci. 5 (2011) 89.
[36] J. Vowinckel, J. Hartl, R. Butler, M. Ralser, MitoLoc: a method for the simultaneous quantification of mitochondrial network morphology and membrane potential in single cells, Mitochondrion 24 (2015) 77–86.
[37] M.D. Abramoff, P.J. Magelhaes, S.J. Ram, Image processing with ImageJ, Biophot. 11 (2004) 36–42.
[38] N.C. Yang, W.M. Ho, Y.H. Chen, M.L. Hu, A convenient one-step extraction of cellular ATP using boiling water for the luciferin-luciferase assay of ATP, Anal. Biochem. 306 (2002) 323–327.
[39] T. MacVicar, T. Langer, OPA1 processing in cell death and disease - the long and short of it, Thomas, J. Cell Sci. 129 (2016) 2297–2306.
[40] A. Signorile, A. Santeramo, G. Tamma, T. Pellegrino, S. D'Oria, P. Lattanzio, D. De Rasmo, Mitochondrial cAMP prevents apoptosis modulating Sirt3 protein level and OPA1 processing in cardiac myoblast cells, Biochim. Biophys. Acta 1864 (2017) 355–366.
[41] A. Jahani-Asl, R.S. Slack, The phosphorylation state of Drp1 determines cell fate, EMBO Rep. 8 (2007) 912–913.
[42] G.M. Cereghetti, A. Stangherlin, O. Martins de Brito, C.R. Chang, C. Blackstone, P. Bernardi, L. Scorrano, Dephosphorylation by calcineurin regulates translocation of Drp1 to mitochondria, Proc. Natl. Acad. Sci. U. S. A. 105 (2008) 1508–15803.
[43] A. Tanaka, R.J. Youle, A chemical inhibitor of DRP1 uncouples mitochondrial fission and apoptosis, Mol. Cell 29 (2008) 409–410.
[44] J.M. Liu, Z. Yi, S.Z. Liu, J.H. Chang, X.B. Dang, Q.Y. Li, Y.L. Zhang, The mitochondrial division inhibitor mdivi-1 attenuates spinal cord ischemia-reperfusion injury both in vitro and in vivo: involvement of BK channels, Brain Res. 1619 (2015) 155–165.
[45] R. Lin, L. Iacovitti, Classic and novel stem cell niches in brain homeostasis and repair, Brain Res. 1628 (2015) 327–342.
[46] M.S. Rao, A.K. Shetty, Efficacy of doublecortin as a marker to analyse the absolute number and dendritic growth of newly generated neurons in the adult dentate gyrus, Eur. J. Neurosci. 19 (2004) 234–246.
[47] M.P. Mattson, M. Gleichmann, A. Cheng, Mitochondria in neuroplasticity and neurological disorders, Neuron 60 (2008) 748–766.
[48] A. Cheng, Y. Hou, M.P. Mattson, Mitochondria and neuroplasticity, ASN Neuro 2 (2010) e00045.
[49] K.H. Flippo, S. Strack, Mitochondrial dynamics in neuronal injury, development and plasticity, J. Cell Sci. 130 (2017) 671–681.
[50] D.C. Chan, Mitochondria: dynamic organelles in disease, aging and development, Cell 125 (2006) 1241–1252.
[51] M. Liesa, B. Borda-d'Agua, G. Medina-Gómez, C.J. Lelliott, J.C. Paz, M. Rojo, M. Palacín, A. Vidal-Puig, A. Zorzano, Mitochondrial fusion is increased by the nuclear coactivator PGC-1 beta, PLoS One 3 (2008) e3613.
[52] L. Lin, M. Zhang, R. Yan, H. Shan, J. Diao, J. Wei, Inhibition of Drp1 attenuates mitochondrial damage and myocardial injury in Coxsackievirus B3 induced myocarditis, Biochem. Biophys. Res. Commun. 484 (2017) 550–556.
[53] N.H. Fukushima, E. Brisch, B.R. Keegan, W. Bleazard, J.M. Shaw, The GTPase effector domain sequence of the Dnm1p GTPase regulates self-assembly and controls a rate-limiting step in mitochondrial fission, Mol. Biol. Cell 12 (2001) 2756–2766.
[54] Q. Wu, C.L. Luo, L.Y. Tao, Dynamin-related protein 1 (Drp1) mediating mitophagy contributes to the pathophysiology of nervous system diseases and brain injury, Histol. Histopathol. 10 (2016) 11841.
[55] H.W. Hyun, S.J. Min, J.E. Kim, CDK5 inhibitors prevent astroglial apoptosis and reactive astrogliosis by regulating PKA and DRP1 phosphorylations in the rat hippocampus, Neurosci. Res. 119 (2017) 24–37.
[56] M. Dierssen, I.F. Vallina, C. Baamonde, S. García-Calatayud, M.A. Lumbreras, J. Flórez, Alterations of central noradrenergic transmission in Ts65Dn mouse, a model for Down syndrome, Brain Res. 749 (1997) 238–244.
[57] S.B. Ong, S. Subrayan, S.Y.D.M. Yellon Lim, S.M. Davidson, D.J. Hausenloy, Inhibiting mitochondrial fission protects the heart against ischemia/reperfusion injury, Circulation 121 (2010) (2012–2022).
[58] M. Khacho, A. Clark, D.S. Svoboda, J. Azzi, J.G. MacLaurin, C. Meghaizel, H. Sesaki, D.C. Lagace, M. Germain, M.E. Harper, D.S. Park, R.S. Slack, Mitochondrial dynamics impacts stem cell identity and fate decisions by regulating a nuclear transcriptional program, Cell Stem Cell 19 (2016) 232–247.
[59] K. Steib, I. Schaffner, R. Jagasia, B. Ebert, D.C. Lie, Mitochondria modify exercise-induced development of stem cell-derived neurons in the adult brain, J. Neurosci. 34 (2014) 6624–6633.
[60] A.A.K. Rosdah, J. Holien, L.M. Delbridge, G.J. Dusting, S.Y. Lim, Mitochondrial fission - a drug target for cytoprotection or cytodestruction? Pharmacol. Res. Perspect. 4 (2016) e00235.
[61] M. Cui, H. Ding, F. Chen, Y. Zhao, Q. Yang, Q. Dong, Mdivi-1 protects against ischemic brain injury via elevating extracellular adenosine in a cAMP/CREB-CD39-dependent manner, Mol. Neurobiol. 53 (2016) 240–253.
[62] J.M. Liu, Z. Yi, S.Z. Liu, J.H. Chang, X.B. Dang, Q.Y. Li, Y.L. Zhang, The mitochondrial division inhibitor mdivi-1 attenuates spinal cord ischemia-reperfusion injury both in vitro and in vivo: involvement of BK channels, Brain Res. 1619 (2015) 155–165.
[63] M.B. Potts, D.A. Lim, An old drug for new ideas: metformin promotes adult neurogenesis and spatial memory formation, Cell Stem Cell 11 (2012) 5–6.